

## Preparation of Well-Defined Hybrid Materials by ATRP in Miniemulsion

Lindsay Bombalski, Ke Min, Hongchen Dong, Chuanbing Tang, and Krzysztof Matyjaszewski\*

Center for Macromolecular Engineering, Department of Chemistry, Carnegie Mellon University, 4400 Fifth Avenue, Pittsburgh, Pennsylvania 15213

Received June 25, 2007

Revised Manuscript Received August 30, 2007

Recent advances in polymer chemistry allow preparation of well-defined organic/inorganic hybrid materials comprising segments that are incompatible at the molecular level.<sup>1</sup> Precise control over the size of each segment permits the formation of materials that display self-organized, nanostructured morphologies with properties suitable for use in a variety of sensing or biomedical applications<sup>2</sup> in addition to preparing materials suitable for reinforcing organic polymers.<sup>3</sup>

The most widely used synthetic route for the preparation of hybrid materials is to conduct a chain growth polymerization from a monolayer of initiators attached to the inorganic particle surface. This “grafting from” approach provides composite structures with the highest grafting density.<sup>4</sup> In particular, atom transfer radical polymerization (ATRP),<sup>5–7</sup> one of the most versatile controlled/living radical processes,<sup>8</sup> has been extensively applied to “grafting-from” procedures, yielding core-shell hybrid particles with controlled thickness of the tethered polymeric shell.<sup>9–11</sup> However, one of the biggest challenges in this approach is to avoid macroscopic gelation resulting from inter-particle coupling reactions.<sup>12,13</sup>

To illustrate the problem arising from cross-linking reactions and/or macroscopic gelation, a bulk ATRP of *n*-butyl acrylate (BA) was carried out using functionalized silica particles as multifunctional initiators (MIs). The MIs were prepared, as previously reported, by reacting 1-(chlorodimethylsilyl)propyl 2-bromoisobutyrate with the hydroxyl groups on the silica particle surface (silica particle diameter  $D = 20$  nm).<sup>20</sup> On the basis of elementary analysis each functionalized silica particle has  $\sim 1600$  initiating sites. The reaction conditions are listed in Table 1, entries 1–5. The silica MIs were dispersed in BA monomer for further ATRP reactions.

The viscosity of the bulk reaction system quickly increased and the stirring bar stopped moving at 25% monomer conversion and at 35% ( $\sim 8.5$  h) the reaction mixture could not form a solution on further dilution, indicating macroscopic gel formation. Since sampling the reaction mixture was not possible after macroscopic gelation, multiple parallel polymerizations were carried out in order to measure the monomer conversions before and after gelation (Table 1, entries 1–5). As seen from the kinetic plot (Figure 1A), the monomer conversion continued to increase even after gelation, demonstrating the “living” character of the systems. Polymerization accelerated after gelation, plausibly due to a slower deactivation at higher viscosity.

On the basis of Flory’s gelation theory for multifunctional systems, a critical gel point should occur when (on average) every multifunctional species is connected to more than two neighbors. Since the average number of initiating sites (func-

tionality) per silica particle was  $\sim 1600$ , the macroscopic gel point should occur when  $2/1600 = 0.125\%$  of the chains terminate in an inter-particle fashion. The amount of terminated chains (including inter- and intra-particle terminations) can be estimated from the radical concentration and the termination coefficient, i.e.,  $\Delta[P_t] = \int k_t[P^*]^2 dt$ . The radical concentration  $[P^*]$  was calculated from the kinetic plot (Figure 1A) to be  $3.8 \times 10^{-10}$  M ( $k_p = 4.82 \times 10^4$  M<sup>-1</sup> s<sup>-1</sup>).<sup>15</sup> Thus, the total number of terminated chains during 8.5 h should be  $10^8$  M<sup>-1</sup> s<sup>-1</sup>  $\times$   $(3.8 \times 10^{-10} \text{ M})^2 \times 8.5 \times 3600 \text{ s} = 4.42 \times 10^{-7}$  M (using an averaged constant value of  $k_t \sim 10^8$  M<sup>-1</sup> s<sup>-1</sup>, although it is recognized that  $k_t$  is not only chain length dependent but also affected by the surrounding of the growing radicals).<sup>16</sup> Since the total concentration of initiating sites was  $1.75 \times 10^{-4}$  M, 0.25% of the chains would have terminated at  $\sim 35\%$  conversion ( $\sim 8.5$  h). This is beyond the calculated gel point, indicating concurrent intra-particle and inter-particle termination reactions.

When the monomer conversion exceeded 35%, the product was partially insoluble in THF due to macroscopic gelation. The fraction of insoluble gel in the reaction flask visibly increased as the reaction progressed, indicating a continuation of the macroscopic gelation process. After the silica particles were etched using HF, the bound polymer was separated and analyzed by GPC. The molecular weights increased linearly with conversion, displaying a narrow molecular weight distribution ( $M_w/M_n$ ), which is evidence of a controlled polymerization, as seen in Figure 1B. It is important to stress that the fraction of chains terminated by coupling (inter- or intra-particle) among all generated polymers was initially not high enough to be detected by GPC (the estimated fraction of the coupled chains was only 0.24% at 8.5 h). However, after  $\sim 50$  h the conversion was essentially complete and the GPC trace of the grafted polymer showed a significant shoulder with molecular weight twice that of the major peak (Figure 1C). This shoulder peak (ca. 20% of all polymers) can be ascribed to radical coupling.<sup>17</sup>

In order to suppress the impact of this inevitable macroscopic gelation, “grafting from” reactions are typically conducted under high dilution,<sup>18,19</sup> over long reaction time<sup>10,20</sup> and/or are stopped at low monomer conversion.<sup>20–22</sup> Another method, based on concurrent polymerization from an unbound “sacrificial” initiator, also efficiently limits inter-particle coupling, plausibly by “diluting” the particles with the free polymer chains with a single functionality which could lead to non-gel forming termination reactions.<sup>19,22</sup> Molecular weights of free and bound polymer are essentially the same.<sup>22,23</sup> In all of these systems gelation could be avoided, producing particles with a uniform polymeric corona. These approaches do therefore minimize inter-particle termination; however, high dilution and low monomer conversion result in solvent and monomer waste and increased cost. The method based on using sacrificial initiator requires the separation of free polymer, which is challenging, especially for very small particles.

An alternative method to suppress inter-particle coupling and macroscopic gelation would be to create boundaries and force polymerization to occur inside very small compartmentalized cells. This “boundary effect” is naturally present in colloidal systems, such as miniemulsion, in which polymerization occurs in separate droplets and multifunctional species cannot react with each other, if they are isolated in different droplets.<sup>24</sup> Although the microscopic cross-linking/gelation can occur inside the droplet, the macroscopic gelation can be efficiently avoided.

\* Corresponding author. E-mail: km3b@andrew.cmu.edu.

Table 1. ATRP of BA from Functionalized Silica Particles in Bulk and Miniemulsion<sup>a</sup>

no.	media	initiation	[BA]:[initiating site]: [Cu]:[L]:[reducing agent]	time (h)	convn (%)	$M_{n,theo}$ (g/mol)	$M_{n,exp}^b$ (g/mol)	$M_w/M_n$
1	bulk	normal	200:1:0.4:0.4:0	8.5	35.9	9190	12 660	1.17
2	bulk	normal	200:1:0.4:0.4:0	12.5	62.5	16 000	18 500	1.16
3	bulk	normal	200:1:0.4:0.4:0	15.5	78.8	20 170	23 170	1.13
4	bulk	normal	200:1:0.4:0.4:0	19.7	91.4	23 400	27 500	1.13
5	bulk	normal	200:1:0.4:0.4:0	51.5	99.9	25 570	38 600	1.60
6	miniemulsion	AGET	200:1:0.4:0.4:0.18	6	51.0	13 050	17 500	1.27
7	miniemulsion	AGET	200:1:0.4:0.4:0.18	6	57.0	14 600	19 000	1.25
8	miniemulsion	AGET	200:1:0.4:0.4:0.18	20	71.4	18 280	24 600	1.16
9	miniemulsion	AGET	200:1:0.2:0.2:0.08	13	80.0	20 480	27 900	1.30

<sup>a</sup> Temp = 80 °C. Ligand: bis(2-pyridylmethyl)octadecylamine (BPMODA).<sup>14</sup> In all normal ATRP systems CuBr was used. In all AGET ATRP systems, CuBr<sub>2</sub> was used together with ascorbic acid as a reducing agent. Miniemulsion conditions: [Brij 98]:[hexadecane] = 2.3/3.6 wt % based on monomer; solids content = 20 wt % (based on 100% conversion). In experiment no. 9, the silica MI had ~1100 initiating sites per particle. <sup>b</sup> Polymers were analyzed by GPC after etching silica with HF.

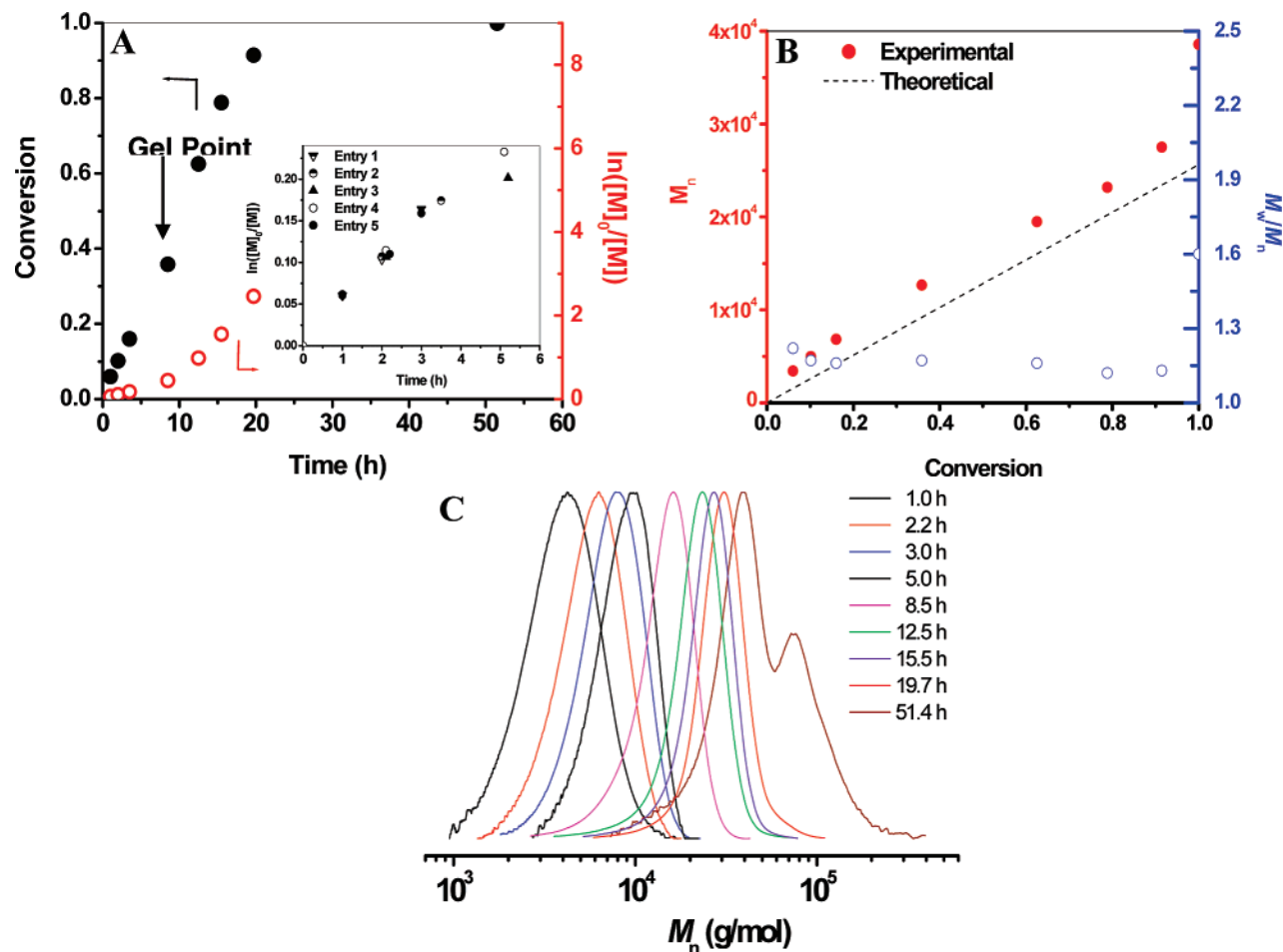


**Figure 1.** (A) First-order kinetic plot of ATRP of BA from silica MIs in bulk. Inset: the first-order kinetic plots during the first 6 h. (B) Evolution of molecular weight of polyBA of hybrid particles vs monomer conversion. (C) GPC traces of cleaved polyBA from bulk ATRP of BA from silica particle MIs. Polymerization conditions: see Table 1, entries 1–5.

Therefore, the “grafting-from” polymerization could attain higher monomer conversion in a miniemulsion process without macroscopic gelation. Herein, we report using this approach for the synthesis of pure (without sacrificial initiator) well-defined hybrid materials: via ATRP of BA from silica particle MIs in an aqueous miniemulsion system.

The initiation technique has to be carefully selected in order to conduct a successful miniemulsion ATRP. A normal ATRP, starting from alkyl halide initiators and Cu(I) activators, is difficult to conduct in a miniemulsion system since either the initiator or catalyst have to diffuse to the dispersed monomer droplets.<sup>25</sup> It is even more challenging in the presence of solid particles, such as silica MIs, that cannot penetrate the droplet

since the MIs cannot be added together with the Cu(I) activators. Distribution of initiator and catalyst was uneven because initiator and catalyst could not be added at the same time. Even after a further sonication process (see Experimental Part in the Supporting Information), the silica MIs cannot be uniformly dispersed throughout the reaction medium. When a series of normal miniemulsion ATRPs were conducted it was found that the polymerization rates varied, suggesting irreproducible concentrations of radicals, plausibly caused by the uncontrolled distribution of silica MIs.

In order to solve the problem of silica particle distribution, a recently developed technique, activators generated by electron transfer (AGET),<sup>25,26</sup> was used for an ATRP miniemulsion

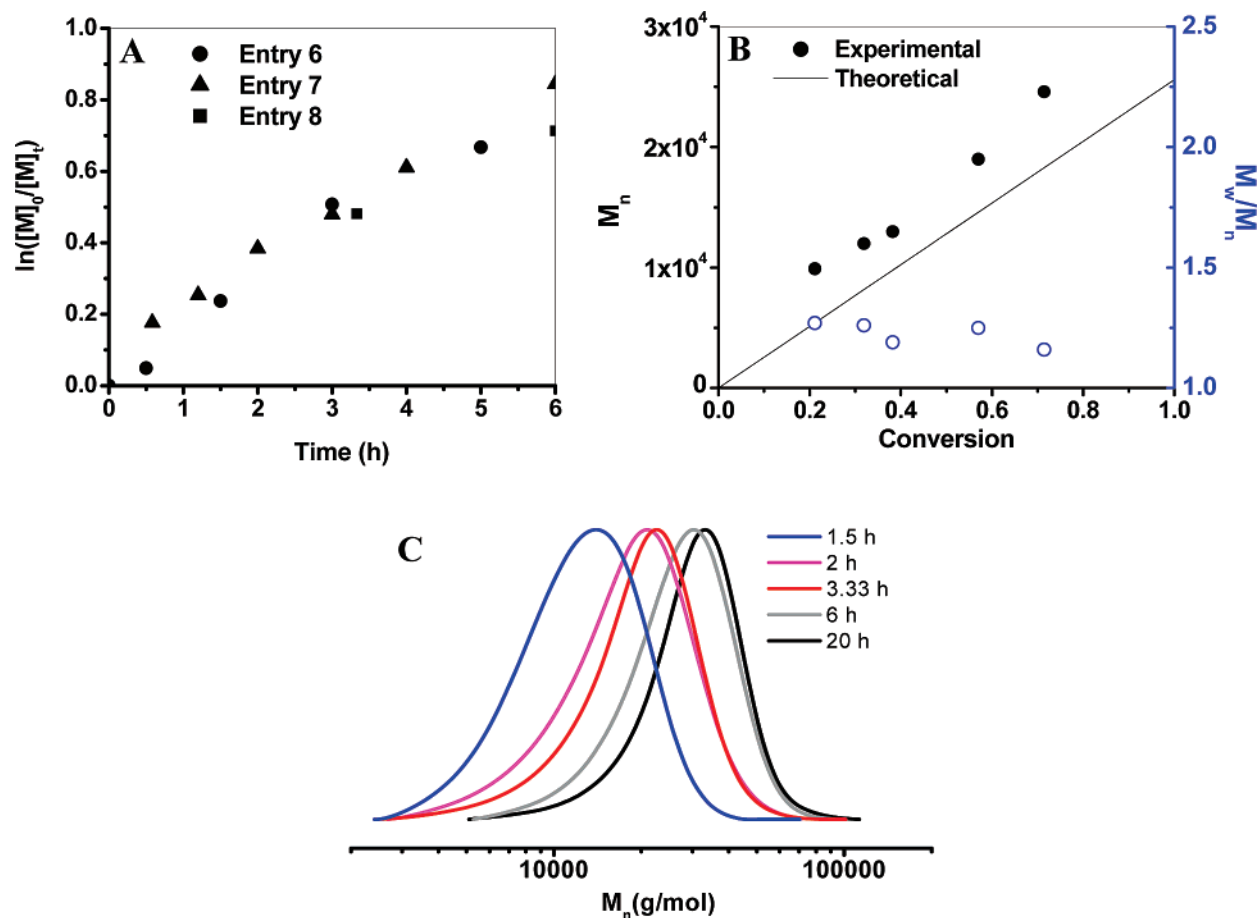


**Figure 2.** (A) First-order kinetic plots for AGET ATRP of BA from silica MI particles in miniemulsion. (B) Evolution of molecular weight of polyBA of hybrid particles vs monomer conversion. (C) GPC traces of polyBA from ATRP of BA from silica MI particles in miniemulsion. Polymerization conditions: see Table 1, entries 6–9.

polymerization from silica MIs. In this procedure, catalyst is introduced in its oxidatively stable state and is subsequently activated by non-radical forming redox reaction with a reducing agent. After activation, the polymerization system is essentially the same as a normal ATRP. Because the catalyst is added in a higher oxidation state and converted in situ to the activator, it can be added together with the macroinitiators and easily survive the sonication procedure. AGET ATRP has been successfully carried out under various heterogeneous conditions.<sup>27–31</sup> In the present study, AGET ATRP was applied to the preparation of hybrid particles in miniemulsion (Table 1, entries 6–9). The reducing agent, ascorbic acid, was added to the system at a sub-stoichiometric amount. The particle size of the miniemulsion was  $220 \pm 10$  nm. In each particle, there were  $\sim 75$  silica particles and  $\sim 120\,000$  growing chain ends (active and dormant).

Compared to the bulk reaction, ATRP in miniemulsion exhibited a higher reaction rate (Figure 2A), most likely due to diffusion of some Cu(II) deactivator species out of the miniemulsion droplets.<sup>25,29,32</sup> According to the kinetic plot,  $[P^*]$  can be calculated as  $9.6 \times 10^{-10}$  M and the concentration of terminated chains in 6 h were estimated to be  $\Delta[P_t] = \int k_t[P^*]^2 dt = 10^8 \text{ M}^{-1} \text{ s}^{-1} \times (9.6 \times 10^{-10} \text{ M})^2 \times 6 \times 3600 \text{ s} = 2.0 \times 10^{-6} \text{ M}$ . Since the concentration of total initiating sites was  $1.75 \times 10^{-4} \text{ M}$ ,  $\sim 1.1\%$  of the chains would participate in termination reactions. As discussed before, the system should form a macroscopic gel when 0.125% of the propagating chains terminate via an inter-particle process. Therefore, in miniemulsion the gelation should have occurred before 6 h. However, in a miniemulsion polymerization inter-particle termination reac-

tions are confined to single droplets and macroscopic gelation is suppressed. In addition, based on the volume of miniemulsion droplet ( $5.57 \times 10^6 \text{ nm}^3$ ), the average number of propagating chains per droplet was only  $5.4 \times 10^{-3}$ . This means, on average 0.54% of droplets were “active” and 99.46% of the droplets were “inactive” with all alkyl halides at the dormant stage.

The miniemulsion remained stable during the entire polymerization. AGET ATRP in miniemulsion reached 70% monomer conversion after 20 h. The molecular weight evolution plot (Figure 2B) shows that high initiation efficiency, 76%, was achieved, comparable to the bulk system. Therefore, miniemulsion media facilitated a faster polymerization and avoided macroscopic gelation.

The miniemulsion AGET ATRP resulted in monomer droplets of  $\sim 220$  nm diameter forming polymer particles, and each of them contained  $\sim 75$  silica-polyBA hybrid particles (each with  $\sim 1600$  chains). After drying the miniemulsion samples, these hybrid particles were individually dispersed in THF and were subject to AFM characterizations. Direct visualization of the core-shell hybrid particles (Figure 3) provides additional evidence for a gel-free system and a controlled miniemulsion ATRP. Random imaging of the other regions on the same substrate surface also indicated a small fraction of particle aggregates in the entire sample. The soft polyBA chains formed a shell with uniform size and can be clearly distinguished from rigid silica cores by AFM. The presence of some free polymer chains (ca. 1%) can result from a small contribution of transfer reactions, chain shear in processing, or residual free initiators remaining after the functionalization of the silica particles.



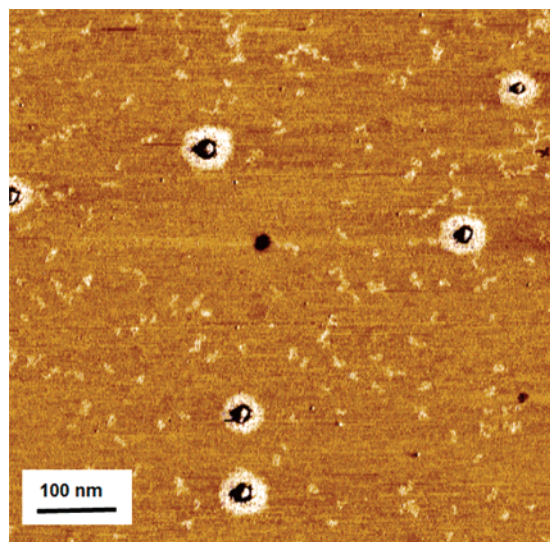


**Figure 3.** AFM image of silica/polyBA hybrid nanoparticles prepared by ATRP in miniemulsion. The hybrid nanoparticles were collected by redispersing the dried miniemulsion samples in THF before subject for AFM characterization. Polymerization conditions: see Table 1, entries 9.

In conclusion, we report the efficient synthesis of hybrid organic/inorganic nanoparticles using silica particles with surface tethered initiators an AGET ATRP miniemulsion process. In comparison to the bulk polymerization, using the same stoichiometry, miniemulsion allowed the preparation of hybrid materials with a higher yield, i.e., higher monomer conversion, and a higher polymerization rate without macroscopic gelation. Direct visualization by AFM provided additional evidence for the formation of well-controlled hybrids. This approach could be applied to the synthesis of various well-defined polymers with complex architectures based on multifunctional initiators.

**Acknowledgment.** Financial support from the CRP Consortium at Carnegie Mellon University and NSF Grants 03-04568 and 05-49353 is greatly appreciated. The authors acknowledge Professor Tomasz Kowalewski for helpful discussions.

**Supporting Information Available:** Text giving the experimental section concerning synthesis and characterization of hybrid nanoparticles. This material is available free of charge via the Internet at <http://pubs.acs.org>.

## References and Notes

- (1) Gravano, S. M.; Patten, T. E. In *Macromolecular Engineering. Precise Synthesis, Materials Properties, Applications*; Matyjaszewski, K., Gnanou, Y., Leibler, L., Eds.; WILEY-VCH: Weinheim, Germany, 2007; Vol. 2.
- (2) Shiflett, M. B.; Foley, H. C. *Science* **1999**, *285*, 1902–1905.
- (3) Merkel, T. C.; Freeman, B. D.; Spontak, R. J.; He, Z.; Pinnau, I.; Meakin, P.; Hill, A. J. *Science* **2002**, *296*, 519–522.
- (4) Edmondson, S.; Osborne, V. L.; Huck, W. T. S. *Chem. Soc. Rev.* **2004**, *33*, 14–22.
- (5) Wang, J.-S.; Matyjaszewski, K. *J. Am. Chem. Soc.* **1995**, *117*, 5614–5615.
- (6) Matyjaszewski, K.; Xia, J. *Chem. Rev.* **2001**, *101*, 2921–2990.
- (7) Tsarevsky, N. V.; Matyjaszewski, K. *Chem. Rev.* **2007**, *107*, 2270–2299.
- (8) Braunecker, W. A.; Matyjaszewski, K. *Prog. Polym. Sci.* **2007**, *32*, 93–146.
- (9) Matyjaszewski, K. *Prog. Polym. Sci.* **2005**, *30*, 858–875.
- (10) Davis, K. A.; Matyjaszewski, K. *Adv. Polym. Sci.* **2002**, *159*, 1–166.
- (11) Von Werne, T.; Patten, T. E. *J. Am. Chem. Soc.* **1999**, *121*, 7409–7410.
- (12) Pyun, J.; Matyjaszewski, K. *Chem. Mater.* **2001**, *13*, 3436–3448.
- (13) von Werne, T. A.; Germack, D. S.; Hagberg, E. C.; Sheares, V. V.; Hawker, C. J.; Carter, K. R. *J. Am. Chem. Soc.* **2003**, *125*, 3831–3838.
- (14) Mori, H.; Seng, D. C.; Zhang, M.; Mueller, A. H. E. *Prog. Colloid Polym. Sci.* **2004**, *126*, 40–43.
- (15) Xia, J.; Matyjaszewski, K. *Macromolecules* **1999**, *32*, 2434–2437.
- (16) Beuermann, S.; Buback, M. *Prog. Polym. Sci.* **2002**, *27*, 191–254.
- (17) Barner-Kowollik, C.; Buback, M.; Egorov, M.; Fukuda, T.; Goto, A.; Olaj, O. F.; Russell, G. T.; Vana, P.; Yamada, B.; Zetterlund, P. B. *Prog. Polym. Sci.* **2005**, *30*, 605–643.
- (18) Yoshikawa, C.; Goto, A.; Fukuda, T. *e-Polym.* **2002**, no. 013.
- (19) Bontempo, D.; Tirelli, N.; Masci, G.; Crescenzi, V.; Hubbell, J. A. *Macromol. Rapid Commun.* **2002**, *23*, 417–422.
- (20) Ohno, K.; Morinaga, T.; Koh, K.; Tsujii, Y.; Fukuda, T. *Macromolecules* **2005**, *38*, 2137–2142.
- (21) Pyun, J.; Jia, S.; Kowalewski, T.; Patterson, G. D.; Matyjaszewski, K. *Macromolecules* **2003**, *36*, 5094–5104.
- (22) Carrot, G.; Diamanti, S.; Manuszak, M.; Charleux, B.; Vairon, J. P. *J. Polym. Sci., Part A: Polym. Chem.* **2001**, *39*, 4294–4301.
- (23) von Werne, T.; Patten, T. E. *J. Am. Chem. Soc.* **2001**, *123*, 7497–7505.
- (24) Tsujii, Y.; Ohno, K.; Yamamoto, S.; Goto, A.; Fukuda, T. *Adv. Polym. Sci.* **2006**, *197*, 1–45.
- (25) Chern, C. S. *Prog. Polym. Sci.* **2006**, *31*, 443–486.
- (26) Sukhorukov, G.; Fery, A.; Moehwald, H. *Prog. Polym. Sci.* **2005**, *30*, 885–897.
- (27) Min, K.; Gao, H.; Matyjaszewski, K. *J. Am. Chem. Soc.* **2005**, *127*, 3825–3830.
- (28) Jakubowski, W.; Matyjaszewski, K. *Macromolecules* **2005**, *38*, 4139–4146.
- (29) Min, K.; Matyjaszewski, K. *Macromolecules* **2005**, *38*, 8131–8134.
- (30) Oh, J. K.; Tang, C.; Gao, H.; Tsarevsky, N. V.; Matyjaszewski, K. *J. Am. Chem. Soc.* **2006**, *128*, 5578–5584.
- (31) Kagawa, Y.; Zetterlund, P. B.; Minami, H.; Okubo, M. *Macromolecules* **2007**, *40*, 3062–3069.
- (32) Min, K.; Oh, J. K.; Matyjaszewski, K. *J. Polym. Sci., Part A: Polym. Chem.* **2007**, *45*, 1413–1423.
- (33) Min, K.; Gao, H.; Matyjaszewski, K. *J. Am. Chem. Soc.* **2006**, *128*, 10521–10526.
- (34) Matyjaszewski, K.; Qiu, J.; Tsarevsky, N. V.; Charleux, B. *J. Polym. Sci., Part A: Polym. Chem.* **2000**, *38*, 4724–4734.

MA071408K